

On the Design of Filter Bank Systems in Power Line Channels Based on Achievable Rate

Francesco Pecile and Andrea Tonello

DIEGM - Università di Udine - Via delle Scienze 208 - 33100 Udine - Italy

phone: +39 0432 558042 - fax: +39 0432 558251 - e-mail: francesco.pecile@uniud.it, tonello@uniud.it

Abstract—We propose a design method for multicarrier systems based on the achievable rate. We focus on pulse-shaped OFDM, adopted by the HomePlug AV system, and filtered multitone modulation (FMT). For a given sub-channel pulse shape, the number of tones and the interpolation factor can be determined by maximizing a design metric based on the achievable rate. Numerical results and comparisons are reported for typical power line communication (PLC) indoor channels, considering also the problem of notching.

I. INTRODUCTION

Multicarrier systems deploy a transmission technique where a high data rate information signal is transmitted through a wide band channel by modulation of a set of parallel signals at low rate. This technique is referred to as multicarrier modulation. The parallel signals are obtained by the serial-to-parallel (S/P) conversion of the input information signal. This idea simplifies the equalization task in highly frequency selective channels that introduce inter-symbol interference (ISI). This is made possible because the wide band channel is divided in a number of narrow band channels that exhibit a nearly flat frequency response when a sufficiently high number of sub-channels is used. If the sub-channels do not exhibit inter-carrier interference (ICI), the equalizer simplifies into a single tap filter.

In this paper we describe a general multicarrier architecture using a filter bank approach in the time domain. This analysis allows discussing several solutions, namely, orthogonal frequency division multiplexing (OFDM) [1], pulse-shaped OFDM [2], filtered multitone modulation (FMT) [3].

Multicarrier modulation is a practical approach to solve the resource allocation problem, i.e., bit and power loading across the sub-channels such that channel capacity is achieved. Assuming to model the system as a set of parallel Gaussian channels, the water filling algorithm provides the optimal power allocation and consequently the number of bits that can be loaded on a given sub-channel can be determined. It should be noted that the achievable rate depends not only on the channel impulse response, and the background noise, but also on the particular prototype pulse used, the number of sub-channels M and the interpolation factor N . In this paper we choose these parameters in order to maximize the achievable rate. As an example, in the case of OFDM, the cyclic prefix

The work of this paper has been partially supported by the European Community's Seventh Framework Programme FP7/2007-2013 under grant agreement n° 213311, project OMEGA - Home Gigabit Networks.

(CP) length has not to be equal to the channel duration to maximize achievable rate [4].

For the numerical examples we focus on the in-home PLC scenario where the channels exhibit severe frequency selectivity in the 0-100 MHz band. This is an extended bandwidth w.r.t. the 0-37.5 MHz band that is used by state-of-the-art systems [5]. It is herein considered to investigate throughput improvements w.r.t. existing technology. In this application scenario the channel among two nodes can be considered static for the duration of one transmission, and several measurement campaigns have shown that the channel duration, is on the order of $5\mu s$ or even longer [6].

We focus on Discrete Fourier Transform (DFT) filter banks, i.e., OFDM and FMT. An analysis of DWMT over PLC channels and a comparison with OFDM is presented in [7].

In this paper we first describe the general system model for DFT filter banks (Section II). In Section III, we deal with FMT, OFDM and pulse-shaped OFDM. Then, in Section IV we address the equalization task and compute the signal-to-noise-plus-interference ratio. In Section V, we discuss the achievable rate as a function of the overhead in the system. In Section VI, we introduce the problem of notching, a fundamental task in the PLC modem design to grant coexistence with other communication systems. In Section VII we discuss numerical results. Finally, the conclusions follow.

II. SYSTEM MODEL

In multicarrier modulation a high rate data signal is split in M parallel data signals $a^{(k)}(\ell T_0)$, $k = \{0, \dots, M-1\}$, where $T_0 = NT$ denotes the sub-channel symbol period assuming a sampling time T in the system. In the most common multicarrier solutions the sub-channel pulse is obtained by the modulation of a prototype pulse. If modulation is accomplished with an exponential function, we have exponentially modulated filter banks. They are also referred to as DFT filter banks, since the efficient implementation is performed using a DFT. Significant examples of DFT filter bank modulation are FMT, OFDM and pulse-shaped OFDM. Each data signal is interpolated by a factor N , filtered with a sub-channel pulse $g(nT)$, and modulated by the k -th sub-carrier $f_k = k/(MT)$. Therefore, the discrete-time multicarrier signal can be written as the output of a synthesis filter bank as follows

$$x(nT) = \sum_{k=0}^{M-1} \sum_{\ell \in \mathbb{Z}} a^{(k)}(\ell T_0) g(nT - \ell T_0) e^{j2\pi f_k nT}. \quad (1)$$

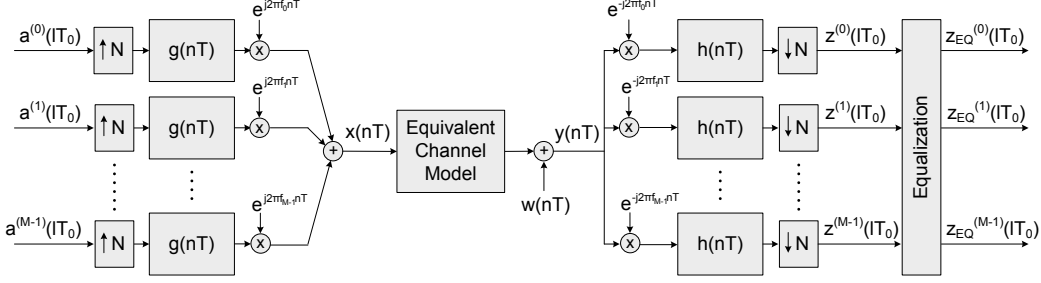


Fig. 1. General scheme for a filter bank based system.

The information data streams $a^{(k)}(\ell T_0)$ belong to the pulse amplitude modulation (PAM), or phase shift keying (PSK), or quadrature amplitude modulation (QAM), constellation sets.

The filter bank modulation scheme is referred to as critically sampled (CS) if $N = M$ while as non-critically sampled (NCS) if $N > M$. We also define the factor $\beta = N - M$ that denotes the amount of overhead used in the multicarrier system, e.g., the cyclic prefix (CP) length in OFDM.

The signal $x(nT)$ is transmitted over a channel with impulse response $g_{CH}(nT)$ and duration L_{CH} (in number of samples) to yield the received signal $y(nT)$. The received signal is analyzed with a filter bank having sub-channel pulses $h(nT)$. The outputs are sampled at rate $1/T_0$ to obtain

$$\begin{aligned} z^{(k)}(\ell T_0) &= \sum_{n \in \mathbb{Z}} y(nT) h(\ell T_0 - nT) e^{-j2\pi f_k nT} \\ &= a^{(k)}(\ell T_0) g_{TOT}^{(k)}(0) + ISI^{(k)}(\ell T_0) \\ &\quad + ICI^{(k)}(\ell T_0) + \eta^{(k)}(\ell T_0), \end{aligned} \quad (2)$$

where $g_{TOT}^{(k)}(0) = g^{(k)} * g_{CH} * h^{(k)}(0)$ is the amplitude of the data of interest, i.e., the overall impulse response of the k -th sub-channel computed at sampling phase zero. Further, we have defined the modulated sub-channel pulses as follows

$$g^{(k)}(nT) = g(nT) e^{j2\pi f_k nT}, \quad h^{(k)}(nT) = h(nT) e^{j2\pi f_k nT}. \quad (3)$$

Besides, $\eta^{(k)}(\ell T_0)$ is the noise term at the sub-channel output, $ISI^{(k)}(\ell T_0)$ and $ICI^{(k)}(\ell T_0)$ denote respectively the inter-symbol and inter-carrier interference components that are in general present when transmitting through a frequency selective channel.

III. FILTER BANK MODULATION SCHEMES

Now, by specializing the prototype filter, we discuss in detail some examples of significant practical interest.

A. Filtered Multitone Modulation

FMT was originally proposed for application in very high speed digital subscriber lines (VDSL) [3]. Then, studied for multiuser wireless communications in [8]. More recently, it has been investigated for power line channels [9]. The sub-channel symbol period is $T_0 \geq MT$ and the analysis pulse is matched to the synthesis pulse, i.e., $h(nT) = g^*(-nT)$. It follows that the overall transmission rate is $R = M/(NT)$ symb/s. A distinctive characteristic of FMT is that the prototype pulse is designed to obtain high frequency confinement [3].

B. OFDM

OFDM [1] is among the most popular multicarrier schemes. It uses the following synthesis pulse

$$g(nT) = \text{rect}\left(\frac{nT}{T_0}\right), \quad (4)$$

while the analysis pulse is

$$h(nT) = \text{rect}\left(-\frac{(n+\mu)T}{MT}\right), \quad (5)$$

where $\mu = N - M$ is the CP length in number of samples, and the rectangular pulse is defined as $\text{rect}(t) = 1$ for $0 \leq t < 1$, and zero otherwise. In this system, the overhead factor β is equal to the CP length. The analysis pulse, that has duration MT , is not matched to the synthesis pulse, whose duration is $T_0 = NT = MT + \mu T$. This is done to cope with the channel time dispersion at the expense of a data rate and signal-to-noise ratio penalty. Also in this system the overall transmission rate is $R = M/(NT)$ symb/s.

C. Pulse-shaped OFDM

Better spectrum confinement can be obtained by substituting the rectangular synthesis pulse in OFDM with a Nyquist window [2]. This yields the pulse-shaped OFDM solution. This choice is adopted by the HomePlug AV (HPAV) system [5]. It can be viewed as an FMT scheme where, however, confinement is privileged in the time domain rather than in the frequency domain. The synthesis sub-channel pulse of (4) is obtained from a prototype pulse that can be for instance a raised cosine pulse (in the time domain) with an integer roll-off α and duration $N + \alpha$ samples, where $T_0 = NT = (M + \mu + \alpha)T$ is the symbol period.

The analysis pulse is

$$h(nT) = \text{rect}\left(-\frac{(n+\mu+\alpha)T}{MT}\right). \quad (6)$$

In this case, under the hypothesis of the same system parameters, a higher overhead β is required than for pure OFDM. In fact, in pulse-shaped OFDM we have that $\beta = N - M = \mu + \alpha$.

IV. EQUALIZATION

We emphasize that ISI and ICI can be mitigated with some form of equalization. The filter bank design aims at reaching a tradeoff between ISI and ICI. While the presence of both ISI and ICI requires a multi-channel equalizer, the presence of

only ISI allows using sub-channel equalization. In our analysis we consider the use of sub-channel equalization only.

Starting from the k -th sub-channel output in (2), we can write an analogous relation at the sub-channel equalizer output

$$\begin{aligned} z_{EQ}^{(k)}(\ell T_0) &= a^{(k)}(\ell T_0)g_{EQ}^{(k)}(0) + ISI_{EQ}^{(k)}(\ell T_0) \\ &\quad + ICI_{EQ}^{(k)}(\ell T_0) + \eta_{EQ}^{(k)}(\ell T_0), \end{aligned} \quad (7)$$

where we use the subscript EQ to denote the dependence from the equalizer. $g_{EQ}^{(k)}(0)$ is the peak of the overall impulse response of the k -th sub-channel at the equalizer output. $\eta_{EQ}^{(k)}(\ell T_0)$ is the noise term at the sub-channel equalizer output. $ISI_{EQ}^{(k)}(\ell T_0)$ and $ICI_{EQ}^{(k)}(\ell T_0)$ denote respectively the residual ISI and ICI components after the equalization stage.

The choice of the proper equalization method depends on the particular filter bank modulation scheme. In FMT the ICI is negligible but some ISI may be present, so sub-channel equalization can be used. Both symbol spaced and more complex fractionally spaced equalization are applicable and considered in this paper to obtain the performance results of Section VII. In pure OFDM and pulse-shaped OFDM, the ICI is present when the CP is shorter than the channel length. However, the optimal CP length has not necessarily to be equal to the channel length to maximize capacity even if single tap equalization is used. This will be shown in the performance analysis (Section VII).

A. Signal-to-Noise-plus-Interference Ratio

To evaluate the performance in terms of achievable rate we need to evaluate the signal-to-noise-plus-interference ratio (SINR) on a given sub-channel at the equalizer output. Looking at (7) we can define it as follows

$$SINR_{EQ}^{(k)}(\beta) = \frac{P_U^{(k)}(\beta)}{P_I^{(k)}(\beta) + P_\eta^{(k)}(\beta)} \quad (8)$$

with

$$P_U^{(k)}(\beta) = E \left[\left| a^{(k)}(\ell T_0)g_{EQ}^{(k)}(0) \right|^2 \right], \quad (9)$$

$$P_I^{(k)}(\beta) = E \left[\left| ISI_{EQ}^{(k)}(\ell T_0) \right|^2 \right] + E \left[\left| ICI_{EQ}^{(k)}(\ell T_0) \right|^2 \right], \quad (10)$$

$$P_\eta^{(k)}(\beta) = E \left[\left| \eta_{EQ}^{(k)}(\ell T_0) \right|^2 \right], \quad (11)$$

computed under the assumption of a static channel (or conditioned on the channel realization). The interference power in (10) can be reduced, increasing implementation complexity, with a proper choice of the equalization procedure. It's worth noting that the SINR is a function of the overhead β . This dependence will be exploited in the next section for the maximization of the achievable rate.

V. ACHIEVABLE RATE AS A FUNCTION OF β

The insertion of the overhead β introduces a loss in the transmission rate that equals $M/(M + \beta)$ where M is the number of sub-channels. In order to evaluate the impact of β on the system performance we compute the achievable rate assuming Gaussian inputs, and additive Gaussian noise to obtain

$$R(\beta) = \frac{1}{T_0} \sum_{k \in K_{ON}} \log_2 \left(1 + \frac{SINR_{EQ}^{(k)}(\beta)}{\Gamma} \right) [bit/s], \quad (12)$$

where K_{ON} is the set of tone indices that are used, i.e., $K_{ON} \subseteq \{0, 1, \dots, M - 1\}$, and Γ represents a gap factor from the Shannon capacity curve that accounts for the deployment of practical modulation and coding schemes. We assume it equal to 3.41 dB when showing numerical results. It corresponds to a target symbol error rate of 10^{-2} with uncoded 1024 QAM [10]. We further assume a power spectral density (PSD) constraint as it is typically the case in power line communications. Therefore, the power is uniformly distributed across sub-channels.

From (12) it is shown that the achievable rate is a function of β . For a fixed number of tones, although the SINR increases as β increases, the data rate decreases. Therefore, the optimal approach to choose β should target the rate maximization. In other words, the optimal β for a given channel maximizes (12), and it is chosen according to

$$\begin{aligned} \beta_{OPT} = \arg \max_{0 \leq \beta \leq L_{CH}} & \left\{ \frac{1}{(M + \beta)} \right. \\ & \times \left. \sum_{k \in K_{ON}} \log_2 \left(1 + \frac{SINR_{EQ}^{(k)}(\beta)}{\Gamma} \right) \right\}. \end{aligned} \quad (13)$$

To obtain a numerical example we consider the statistical PLC channel model presented in [11] that is representative of indoor PLC channels. The bandwidth is fixed at $1/T = 100$ MHz, and the impulse response is truncated at $5.56\mu s$, which corresponds to 556 samples. From now on we assume a constant transmit PSD mask equal to -50 dBm/Hz and an additive Gaussian noise with PSD equal to -140 dBm/Hz. The channel is normalized such that the average attenuation over the 0-100 MHz band is equal to 46, 66 or 86 dB. Therefore, the average SNR at the receiver equals 44, 24 or 4 dB. The average path loss profile matches typical values measured in in-home networks [6].

In Fig. 2 an example of typical PLC indoor channel impulse response is depicted. It has been chosen with a procedure analogous to the one described in [4]. It corresponds to the worst channel realization obtained from the statistical channel model considered in [6], [11]. This realization will be used for all the numerical results herein reported.

In Fig. 3 we plot the achievable rate defined in (12) as a function of the overhead β . We consider FMT and pulse-shaped OFDM. We omit pure OFDM since the behavior is similar to that of pulse-shaped OFDM and significantly worse

when notching is applied. The systems have $M = 1024$ subcarriers, and the set of the used tones is $K_{ON} = \{21, \dots, 1024\}$ to operate in the band 2-100 MHz. Although it is not shown due to space limitations, the SINR increases as the overhead increases and reaches the maximum when β equals the channel duration (556 samples) for both systems. However, the achievable rate curves show that the maximum is reached for β shorter than 556 samples. Further, the lower the SNR the smaller the factor β that maximizes rate is. This behavior is justified by the fact that for high SNRs the performance is dominated by the interference.

Looking at Fig. 3 we can notice that the achievable rate is a function of the SNR. Further, the rate gain is a function of the affordable receiver complexity. In pulse-shaped OFDM single tap sub-channel equalization is deployed. In FMT an identical equalization scheme can be used (labeled with Equal. 1 Tap). Since FMT exhibits sub-channel ISI, significant improvements can be obtained with more complex equalization. Herein, we have considered MMSE fractionally spaced sub-channel equalization with a number of taps equal to 2, 10 and 20 (labeled with FS Equal. 2, 10, 20 Taps). More than 20 taps do not yield significant improvements. It should be noted that in the FMT system the choice of β_{OPT} , for a given SNR value, is not influenced by the equalization method.

We finally remark that the practical implementation requires estimation of the sub-channels SINR at the receiver, and feedback to the transmitter of the overhead β_{OPT} .

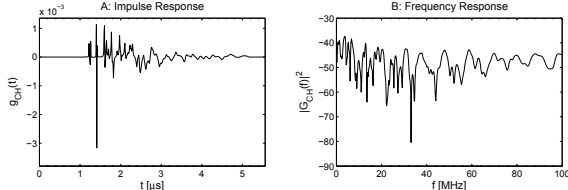


Fig. 2. Realization of PLC channel impulse response and frequency response.

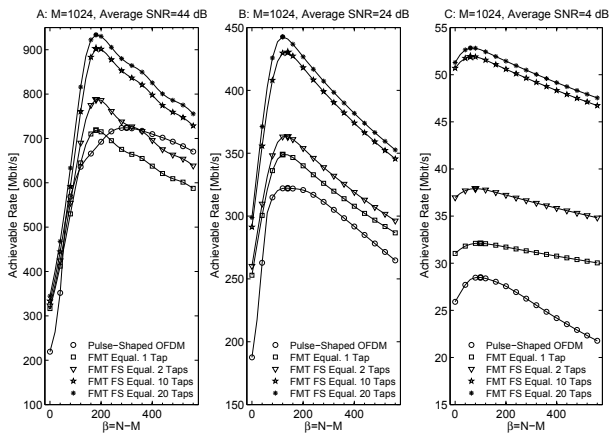


Fig. 3. Achievable rate as a function of the system overhead β .

VI. NOTCHING

The coexistence with other technologies implies that the PLC PHY shall be robust to interference and shall also generate low radiations in certain parts of the spectrum. The main sources of interference in the 0-37.5 MHz frequency

band are the radio amateur signals and the AM broadcasters. A robust approach to allow the coexistence is to notch the emitted signal at certain frequencies. The multicarrier schemes that deploy frequency confined sub-channel pulses can obtain higher notch selectivity, i.e., fewer tones have to be switched off to fulfill the mask, and consequently they experience lower loss in data rate. In the next section we discuss the achievable rate in the presence and the absence of notching for FMT modulation and for pulse-shaped OFDM. We assume the notching mask of Fig. 4. In the 0-30 MHz band we apply the mask described in [12], which is similar to that used by the HomePlug AV system, while we do not operate any notching in the 30-100 MHz band. Further notching can be done beyond 30 MHz to grant coexistence with other communication systems.

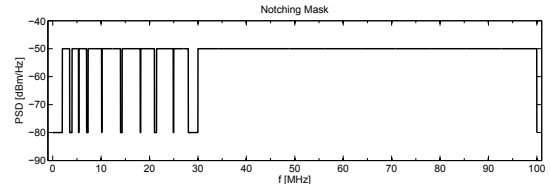


Fig. 4. PSD mask in the 0-100 MHz band.

VII. PERFORMANCE

In the following we report the numerical results for pulse-shaped OFDM and FMT. We assume the same system parameters of Section V. The channel impulse response of Fig. 2 is considered. The average SNR at the receiver, after channel attenuation, equals 44, 24 or 4 dB. It should be noted that the interference in the computation of the SINR includes the narrow band interference, the ISI and the ICI. We report in Fig. 5 and Fig. 6 the achievable rate in (12) as a function of the total number of system tones, that is equal to $M = \{256, 512, 1024, 2048, 4096\}$.

The achievable rate for the unmasked case (Fig. 5) is obtained by switching off only the tones at the band edges to obtain an effective transmission band in 2-100 MHz. The achievable rate for the masked case (Fig. 6) is obtained by switching off extra tones such that the mask of Fig. 4 is satisfied. Pulse-shaped OFDM has better spectral confinement than pure OFDM if it deploys a raised-cosine window with roll-off equal to $CP/2$, as herein considered. Significant improvements in the sub-channel confinement are obtained with FMT that uses a truncated root-raised-cosine pulse with roll-off 0.2 and length $12T_0$. The interpolation factor N and the CP length have been selected via rate maximization as described in Section V.

Now looking at Fig. 5 and Fig. 6, we can notice that FMT achieves higher rate than pulse-shaped OFDM both for the masked and the unmasked case. It is interesting to note that the lower the SNR is, the higher is the advantage of FMT w.r.t. pulse-shaped OFDM. Moreover, even for very low SNRs the achievable rate is relatively high. For the masked case single tap equalization in FMT outperforms pulse-shaped OFDM for an SNR equal to 24 and 4 dB and for all the number of

tones herein considered. This is due to the excellent frequency confinement of FMT, that corresponds to a better notching capability.

For a practical number of tones values, pulse-shaped OFDM has worse performance than FMT since it uses more redundancy, it suffers for an SNR loss, and requires notching a higher number of tones to fulfill the imposed PSD mask. Interestingly, FMT achieves the maximum rate with a smaller number of tones provided that equalization is performed (equal to 1024 in the scenario considered). In turn, this allows lowering the implementation complexity.

In Fig. 7 we plot the achievable rate for the masked case in the 2-28 MHz band. The results are obtained selecting the proper set of carriers K_{ON} in the computation of (12), i.e., we apply the mask described in [12] in the 2-28 MHz band and we switch off all the tones in the 28-100 MHz band. The average SNR reported in the plots is the one computed over the 0-100 MHz bandwidth, as previously described. Comparing Fig. 6 with Fig. 7 we can determine the increase in achievable rate that is attainable when increasing the bandwidth from 28 MHz to 100 MHz. The achievable rate roughly scales linearly with the band, i.e., it increases by a factor from 2 to 3 depending on the SNR. Moreover, also in this scenario FMT with single tap equalization significantly outperforms pulse-shaped OFDM.

VIII. CONCLUSION

We have investigated the problem of designing multicarrier systems to maximize achievable rate. In particular, for a given prototype pulse and number of tones, the overhead, i.e., interpolation factor or cyclic prefix that maximizes the achievable rate is less than the channel length. The results show that the achievable rate can be used as a metric to choose properly the number of carriers and the equalization method in the system such that a tradeoff between performance and complexity is accomplished. Further, the parameters can be adapted to the specific channel realization, or following the methodology herein described we can determine a globally optimal set of parameters for typical PLC channels.

REFERENCES

- [1] S. Weinstein and P. Ebert, "Data Transmission by Frequency-Division Multiplexing Using the Discrete Fourier Transform," *IEEE Transactions on Communication Technology*, vol.19, no.5, pp.628-634, October 1971.
- [2] F. Sjoberg, R. Nilsson, M. Isaksson, P. Odling and P.O. Borjesson, "Asynchronous Zipper," *IEEE International Conference on Communications*, ICC 1999, vol.1, pp.231-235, 6-10 June 1999.
- [3] G. Cherubini, E. Eleftheriou and S. ÖLcer, "Filtered Multitone Modulation for Very High-Speed Digital Subscriber Lines," *IEEE J. Sel. Areas Commun.*, vol.20, no.5, pp.1016-1028, June 2002.
- [4] A.M. Tonello, S. D'Alessandro and L. Lampe, "Bit, tone and cyclic prefix allocation in OFDM with application to in-home PLC," *IEEE IFIP Wireless Days 2008*, 24-27 November 2008.
- [5] HomePlug AV System Specifications, Version 1.0.09, Feb. 2007.
- [6] OMEGA project deliverable D3.2 "PLC Channel Characterization and Modelling," available at: http://www.ict-omega.eu/fileadmin/documents/deliverables/Omega_D3.2.pdf.
- [7] S. Galli, H. Koga and N. Kodama, "Advanced Signal Processing for PLCs: Wavelet-OFDM," *IEEE International Symposium on Power Line Communications*, ISPLC '08, pp.187-192, 2-4 April 2008.
- [8] A.M. Tonello, "Asynchronous Multicarrier Multiple Access: Optimal and Sub-Optimal Detection and Decoding," *Bell Labs Tech. Journal*, special issue: Wireless Radio Access Networks, vol.7, no. 3, pp.191-217, 2003.
- [9] A.M. Tonello and F. Pecile, "Efficient architectures for multiuser FMT systems and application to power line communications," *IEEE Transactions on Communications*, in press.
- [10] J.M. Cioffi, Advanced Digital Communication, chapter 4, available at: <http://www.stanford.edu/class/ee379c/reader.html>.
- [11] A.M. Tonello, "Wideband Impulse Modulation and Receiver Algorithms for Multiuser Power Line Communications," *EURASIP Journal on Advances in Signal Processing*, vol. 2007, pp.1-14.
- [12] K.H. Afkhamie, H. Latchman, L. Yonge, T. Davidson and R. Newman "Joint Optimization of Transmit Pulse Shaping, Guard Interval Length, and Receiver Side Narrow-band Interference Mitigation in the HomePlugAV OFDM system," *IEEE 6th Workshop on Signal Processing Advances in Wireless Communications*, pp.996-1000, 5-8 June 2005.

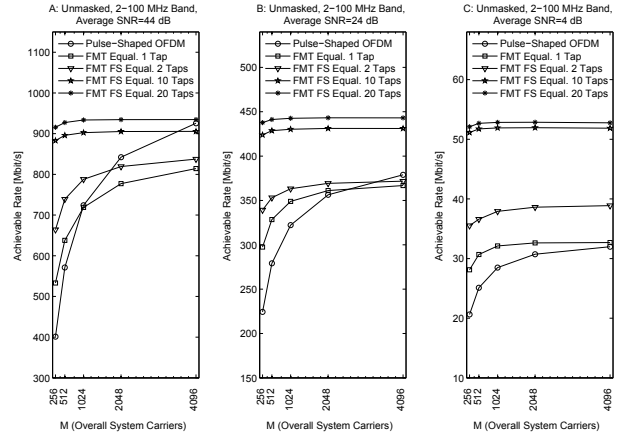


Fig. 5. Achievable rate comparison. Unmasked case in the 2-100 MHz band.

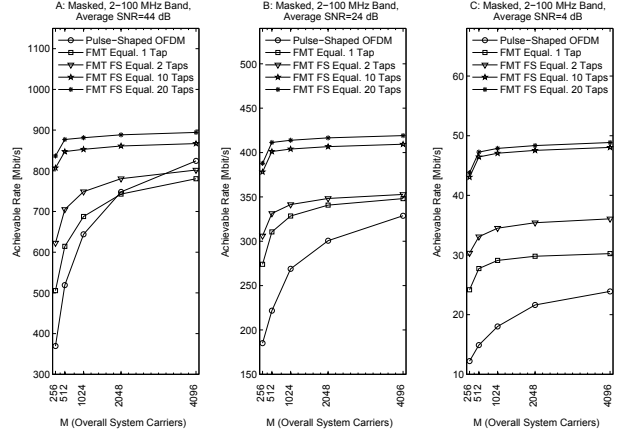


Fig. 6. Achievable rate comparison. Masked case in the 2-100 MHz band.

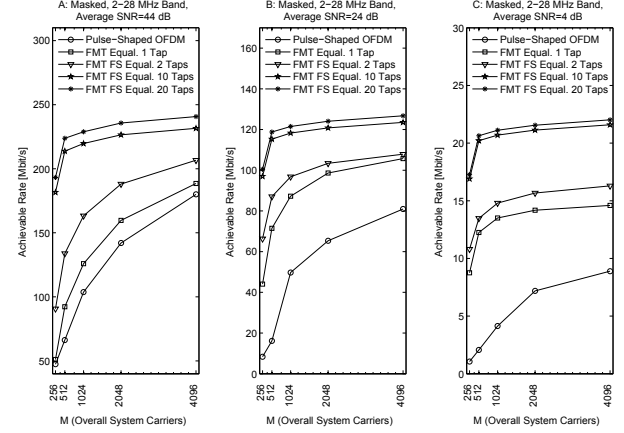


Fig. 7. Achievable rate comparison. Masked case in the 2-28 MHz band.